CARDIFRC® - Properties and application to retrofitting

S.D.P. Benson & B.L. Karihaloo

Cardiff University, Cardiff, UK

F.J. Alaee

Shahrood University of Technology, Shahrood, Iran

ABSTRACT: This paper will describe first the important steps necessary for the manufacture of the high performance fibre reinforced cementitious composite developed at Cardiff University. These steps have been patented (GB 0109686.6) and the class of materials so produced registered under the trademark CARDIFRC®. It will then describe a new technique of retrofitting damaged and/or understrength RC beams. In this technique thin pre-cast strips of CARDIFRC® are adhesively bonded to the tension face and, if necessary, other faces of the beams. This technique ensures that the ultimate failure of the retrofitted beams will occur in the gradual flexural mode. It therefore overcomes some of the problems encountered with the existing techniques, based on externally bonded steel plates and FRP laminates, which arise primarily due to the mismatch of their tensile strength and stiffness with that of concrete.

The paper will then outline two analytical/computational models for predicting the ultimate moment capacity and the complete load-deflection behaviour of retrofitted RC beams. The first model takes a classical approach involving the tensile contribution from the reinforcing steel and the compressive contribution from concrete, but it also includes the complete tensile contribution of concrete and of the retrofit CARDIFRC® strips. The second computational model takes a purely fracture mechanics approach and follows the initiation and growth of the dominant flexural crack that eventually leads to the failure of the retrofitted beams.

Both computational models predict ultimate moment capacity and load-deflection behaviour that are in excellent agreement with test results.

Keyword: RC beams, retrofitting, high performance FRC, adhesive bonding, computational modelling, ultimate moment capacity.

1. INTRODUCTION

A new technique of retrofitting damaged and/or understrength reinforced concrete beams has been recently developed by the authors. In this technique thin, pre-cast strips of high-performance fibre-reinforced cementitious composite, also developed at Cardiff and designated CARDIFRC®, are adhesively bonded to the tension and, if necessary, other faces of the RC beam. This technique ensures that the ultimate failure of the retrofitted beams will occur in the gradual, flexural mode. It therefore overcomes some of the problems associated with the existing retrofitting techniques, based on externally bonded steel plates and FRP laminates, which arise primarily due to the mismatch of their tensile strength and stiffness with that of concrete.

The performance of current techniques of rehabilitation and strengthening (the collective term retrofit, which implies the addition of structural components after initial construction, captures both rehabilitation and strengthening) using externally bonded steel plates and fibre-reinforced plastic (FRP) laminates has been extensively investigated (Ahmed and Gemert, 1999; El-Refaie et al., 1999). The technique of retrofitting using externally bonded steel plates has gained widespread popularity, being quick, causing minimal site disruption and producing only minimal change in section size. However, several problems have been encountered with this technique, including the occurrence of undesirable

shear failures, difficulty in handling heavy steel plates, corrosion of the steel, and the need for butt joint systems as a result of limited workable lengths.

FRP materials as thin laminates or fabrics would appear to offer an ideal alternative to steel plates. They generally have high strength to weight and stiffness to weight ratios and are chemically quite inert, offering significant potential for lightweight, cost effective and durable retrofit (Nanni, 1995; Büyüköztürk and Hearing, 1998). Retrofitting using FRP is also vulnerable to undesirable brittle failures due to a large mismatch in the tensile strength and stiffness with that of concrete.

CARDIFRC® is a fibre reinforced cementitious composite which is characterised by high tensile/flexural strength and high energy-absorption capacity (i.e. ductility). The special characteristics of CARDIFRC® make it particularly suitable for repair, remedial and upgrading activities (i.e. retrofitting) of existing concrete structures. The key advantage of CARDIFRC® mixes for retrofitting is that unlike steel and FRP, their tensile strength, stiffness and coefficient of linear thermal expansion are comparable to that of the material of the parent member. Two typical optimum mix proportions of CARDIFRC® (Mix I and Mix II) are given in Table 1, with the typical material properties shown in Table 2.

Several studies have previously been undertaken at Cardiff into the feasibility of using CARDIFRC® for the rehabilitation and strengthening of damaged RC flexural members (Karihaloo et al., 2002, 2000; Alaee et al., 2002). To predict the moment resistance and the load-deflection behaviour of the beams retrofitted with CARDIFRC® two analytical models have been developed (Alaee and Karihaloo, 2003a, 2003b). One model is based on the classical strength theory, but takes into account fully the tensile contributions (i.e. pre-peak and post-peak) from concrete and CARDIFRC®. The second analytical model is based on fracture mechanics concepts. This model mimics the initiation and growth of the flexural crack that eventually leads to the failure of the retrofitted beam.

Both computational models predict ultimate moment capacity and load-deformation behaviour that are in excellent agreement with test results. It is also shown that such an agreement would not have been possible without the inclusion of proper tension softening response of both concrete and CARDIFRC®, thus demonstrating conclusively the importance of fracture mechanics concepts to the design of RC structures.

Table 1. Mix Proportions for optimised CARDIFRC® Mix I and Mix II (per m^3).

Constituents (kg)	Mix I	Mix II
Cement	855	744
Microsilica	214	178
Quartz sand:		
9-300μm	470	166
250-600μm	470	-
212-1000μm	-	335
1-2mm	-	672
Water	188	149
Superplasticiser	28	55
Fibres: - 6mm	390	351
- 13mm	78	117
Water/cement	0.22	0.20
Water/binder	0.18	0.16

Table 2. Typical Material Properties of CARDIFRC® Mix I and Mix II.

Material properties	Mix I	Mix II
Indirect tensile strength (MPa)	24	25
Fracture energy (J/m^2)	17,000	21,000
Compressive strength (MPa)	207	185

2. PROPERTIES OF CARDIFRC®

Exhaustive rheological studies have been carried out in Cardiff to optimise HPFRCCs. The aim was to achieve good workable mixes with a very low water/binder ratio and a high volume fraction of steel fibre, in order that the resulting material, in its hardened state, will be very ductile with a relatively high tensile strength. This has resulted in a range of mixes being developed. Two different mixes (designated CARDIFRC®, Mix I and Mix II) differing mainly by the maximum size of quartz sand used in the mix obtained using novel mixing and fibre dispersion procedures are shown in Table 1. These procedures are described in the patent application GB 0109686.6.

Brass-coated steel fibres diameter 0.16mm, 6mm or 13mm long are used to prevent corrosion. The optimised grading of quartz sands leads to a considerable reduction in the water demand without loss in workability. All materials used in Table 1 are available commercially.

A volume fraction of 6% short and long fibres is used, comprising 5% short fibres and 1% long fibres for Mix I, and 4.5% short fibres and 1.5% long fibres for Mix II. The specimens were hot-cured at 90°C for seven days. The strengths attained have been found to be the equivalent of standard 28-day water curing at 20°C. Table 2 shows the material properties of the optimised

mixes. The Young Modulus of CARDIFRC® is around 50GPa.

3. EVOLUTION OF MICROCRACKS

The strain hardening behaviour of CARDIFRC® is due to the nucleation of microcracks under increasing tensile/flexural stress (Karihaloo et al., 1996; Wang et al., 2000; Karihaloo & Wang, 2000). In the literature, assumptions have been made on their evolution but no experimental evidence is available to validate them. An experimental programme was implemented to quantify the increase in crack density ω as a function of the applied tensile stress σ and fibre parameters. For this it was necessary to use a specimen geometry with a uniform tensile stress field over a large area which is unaffected by the loading arrangement. The specimen shown in Figure 1 ensures a central area in which the tensile stress is uniform and well defined. The geometry was determined as follows.

Based on Neuber's formula (Neuber, 1969) for a precise spline geometry with no stress concentrations, finite element analysis was used to develop a modified spline that would ensure a smaller central area of uniform stress. This was necessary to reduce the scanning area of the CCD (charge-coupled device) camera for crack observation. This geometry was realised by feeding the exact co-ordinates into a numerically-controlled lathe which produces timber cut outs.

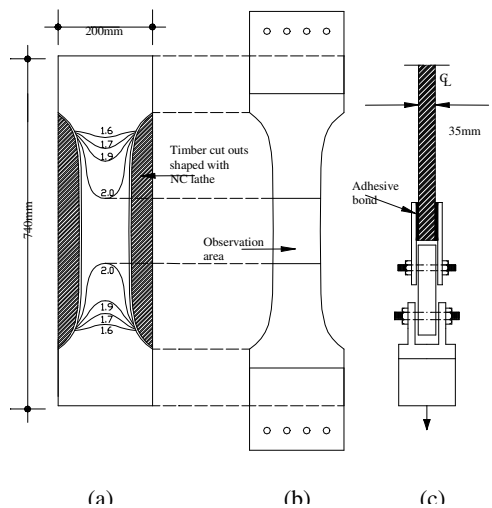

Figure 1. Special tensile specimen geometry, showing (a) contours of tensile stress under a unit external tension, (b) the observation area with a uniform and well-defined tension field and (c) the load application arrangement.

The latter were positioned in a rectangular steel mould, as shown in the figure. The mould was then filled with the test CARDIFRC® mix and compacted on a vibrating table. The middle third of the flat surfaces of the specimen was coated with a brittle coating. The specimen was loaded gradually in tension through the loading arrangement shown in the figure and its coated surfaces were scanned by the CCD camera for evidence of microcracks. As the length of microcracks is approximately equal to the maximum size of quartz sand used in the mix, a CCD camera coupled with a high magnification optical lens (x 60) is needed for this purpose. The CCD camera was mounted on a frame that enabled the camera to be moved in the x- and y-direction. The camera scanned the area of uniform stress for microcracks under increasing tensile loading. This process was continued until the microcracks localised into macrocrack(s) in the eventual fracture plane, i.e. until the peak load was reached.

The novel test specimen profile proved very effective in providing a specific area of uniform tensile stress to facilitate the observation of crack evolution and propagation without inducing a bias into the location of crack initiation. Results show that the fracture process zone is not due to one dominant crack but is due to many cracks. In support of this, parallel cracks, crack branching, cracks linking-up and multiple cracking were all observed and recorded. In addition, as the active crack opens, evidence of fibre bridging was confirmed. It was also noted that not all cracks continued to propagate; some cracks became dormant since the failure plane will occur along the path of least resistance. Tests show only small differences in the mechanical properties between the two types of mix (CARDIFRC® mix I and mix II) and the specific fracture energy values were in excellent agreement with those found by indirect flexural tests modified to be size independent (Table 2). The specific fracture energy was found to be in the region of 17,000 to 20,500N/m and the uniaxial tensile strength was between 12 and 13.5MPa.

Numerical expressions have been fitted to the test data to describe each of the three regions. The three regions predicted by the equations can be seen in Figure 2. Laboratory test work shows clear evidence that the linear elastic region is larger than theoretically predicted (Karihaloo & Wang, 2000), a smaller strain hardening region with a distinct plateau at the peak load followed by a gradual decrease in the stress after the peak load.

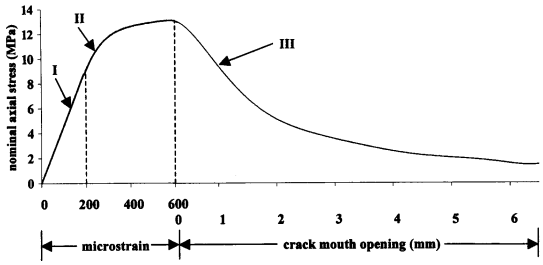

Figure 2. Complete pre- and post-peak tensile curve for CARDIFRC® as prescribed by Equations (1) to (3).

- REGION I – Linear-elastic region
  Applicable from 0 to 200 microstrain

  • = 0.046• (1)

  giving the Young modulus value of 46GPa.
- REGION II – Strain hardening region
  Applicable from 200 to 600 microstrain

  • = $-4.34*10^{-10}$• ^{4} + $8.315*10^{-7}$• ^{3} – $6.03*10^{-4}$• ^{2} + 0.199• -12.619 (2)

- REGION III – Tension softening region
  Applicable from 0.22 to 6.5mm crack mouth opening (w)

  • = $3.069107*10^{-3}w^7 - 0.078952w^6 + 0.822382w^5 - 4.420119w^4 + 12.797151w^3 - 18.105342w^2 + 5.732789w + 12.894413$ (3)

When comparing the above approximations with the experimental results, the approximate polynomials were practically indistinguishable from the test data.

4. WORKABILITY OF CARDIFRC®

Traditional workability tests, namely slump and Vebe time, are not suitable for testing the CARDIFRC® matrix, which is an extremely fluid mix in the absence of fibres. These tests were designed for much stiffer mixes. The mix constituents of CARDIFRC® make it more like a sandy soil because it consists of graded sand and smaller particles in the form of cement and microsilica. The cone penetrometer test (CPT), a test designed for determining the liquid limit of a soil, is suitable for measuring the workability of the CARDIFRC® matrix. The standard apparatus and measurement procedure was used. Constant workability of the mixes, as measured by the cone penetration, was ensured by adjusting the amount of superplasticizer. Penetration values of 20, 22 and 24mm were chosen as the three target values to be achieved for each of the mixes made. The maximum penetration measurable from the CPT is 25mm; the matrix for CARDIFRC® approaches this limit easily, hence three lower values were chosen. This provides us with three fixed targets for workability. For each target value, the workability was quantified by measuring the fracture toughness $\kappa_{Ic,m}$ of the mix.

5. DISTRIBUTION OF FIBRES

To ensure that the mixing and compaction procedures do indeed result in an even and random distribution of fibres in the hardened CARDIFRC® both destructive and non-destructive techniques were employed.

For non-destructive evaluation of the fibre distribution computer tomography (CT) imaging technique was used. CT imaging is a technique whereby cross-sectional images are generated by computer software from multiple X-ray readings. The amount of the X-ray beam transmitted through the object as it is continuously moved through the stator of the scanner is measured, in all directions around the 360° stator, and the X-ray attenuation, measured in Hounsfield units, calculated. The images are compiled from thousands of readings taken in the different directions using a computer program based on an image reconstruction algorithm. This idea was first introduced for plain concrete by Karihaloo and Jefferson (2001) and has been extended to study the influence of mixing and compaction procedures on the distribution of fibres in various specimens (namely, tensile specimens, thin strips, small beams, cylinders and cubes).

The CT images are produced by mapping the X-ray absorption density in Hounsfield units onto a grey scale, such that air appears black (-1000 Hounsfield units) and the densest particles in the specimen appear white (3017 Hounsfield units) with water being calibrated at 0 Hounsfield units. As even the latest CT helical scanners are unable to resolve individual steel fibres because of their small diameter (0.15mm), it was decided to produce contour plots of the X-ray absorption density at 2 or 3 sections along the length of each specimen. The specimen could subsequently be cut along these sections and the fibre distribution analysed by image analysis. In this way, the X-ray absorption density contours can be correlated to the actual fibre distribution.

6. TEST BEAMS

Two types of beam differing only by the reinforcement were used for stages I and II of the experimental programme. The beams in stage I were reinforced in flexure only with a single 12mm rebar, whereas in the beams tested in stage II, stirrups were also provided in the shear spans of the beams. All the beams were made from a standard concrete mix and were 1200mm long, 100mm wide and 150mm deep.

6.1 Stage I

Of the thirty-two beams used in stage I, four were tested to failure as control beams to compare with the performance of those retrofitted with CARDIFRC® strips. The remaining twenty-eight beams were pre-loaded to approximately 75% of the above failure load to induce flexural cracking. In addition to parameters such as the material (Mix I or II) and thickness of retrofit strips (16 or 20mm), four different configurations of retrofitting were investigated.

6.2 Stage II

Of the fourteen beams produced for stage II, three were tested without any repair as control beams. These beams were tested to failure under four-point bending over a span of 1100mm. The spacing between the applied loads was 400mm. The remaining eleven beams were pre-loaded in the same manner as the control beams to approximately 75% of the failure load. To improve the flexural behaviour of the damaged beams three configurations of retrofitting strips were investigated in this stage.

6.3 Casting of Strips

The retrofit materials, CARDIFRC® Mix I and Mix II were cast as flat strips in 1030mm long and 100mm wide steel moulds with a well-oiled base and raised border whose height could be adjusted to give 16 or 20mm thick plates. The moulds were filled on a vibrating table at 50Hz frequency and smoothed over with a float. To ensure a uniform thickness (within 1mm) a glass panel was located on top of the raised border. The strips were left to cure in the moulds for 24 hours at 20°C before de-moulding. The retrofit strips were then hot-cured at 90°C for a further 9 days (including one day for raising and one day for lowering the temperature). The short rectangular and trapezoidal side strips for shear strengthening, were cut from the long cast strips to the required size using a diamond saw.

6.4 Adhesive bonding

To improve the bond between the retrofit strips and the damaged beams, all contacting surfaces were carefully cleaned and roughened. An angle grinder was used to create a grid of grooves approximately 3mm deep at a spacing of 50mm on the contacting surfaces of the damaged beams.

The retrofit strips were bonded to the prepared surfaces of the damaged concrete beams with a commercial thixotropic epoxy adhesive. The two parts of the adhesive were thoroughly mixed and applied to the tension side of the damaged beam with a serrated trowel to a uniform thickness of 3mm. The strips were placed on the adhesive and evenly pressed. To ensure good adhesion, pressure must be applied to the strips during the hardening of the adhesive (24 hours) in accordance with the manufacturer's recommendation.

For the retrofitted beam with more than one strip, the beam was turned on its side to which the strip was bonded in the same manner as above. After another 24 hours, this procedure was repeated on the other side of the damaged beam. In practice, to ensure good adhesion between the strips and the damaged beam pressure can be applied using G-clamps.

7. FIRST ANALYTICAL MODEL

To predict the moment resistance and the load-deflection behaviour of the control and retrofitted beams two analytical models have been developed. In the first model the strain hardening as well as tension softening of both concrete and CARDIFRC® in tension have been taken into account. The stress-strain relationships of materials were assumed to be according to the test results or the proposed stress-deformation diagrams of the Model Code CEB-FIP (1993). Based on this code, steel is assumed to be perfectly elasto-plastic, whereas a parabolic relation is used for concrete in compression. For concrete, the compressive strength was measured experimentally, and the remaining parameters were calculated from the relations proposed by CEB-FIP. The yield stress f_y and the modulus of elasticity E_s of steel were obtained from tension test on rebars.

Tensile failure of concrete and CARDIFRC® is always a discrete phenomenon. Therefore, to describe this behaviour a stress-strain and a stress-crack opening relation should be used for the uncracked and cracked sections, respectively. For normal concrete in tension the stress-deformation behaviour proposed by CEB-FIP was assumed,

whereas the behaviour of CARDIFRC® in tension was modelled based on the theory of fracture mechanics and available test results. For concrete, the direct tensile strength f_{ctm} was estimated from the splitting test results and the remaining parameters were again calculated from the relations proposed by CEB-FIP. For CARDIFRC® the tensile strength of the matrix f_{tp} was estimated from the splitting test results of the mix without fibres. However, the specific fracture energy G_F and the modulus of elasticity E were directly measured using the notched beam and prism specimens, respectively.

The moment resistance of a section retrofitted by CARDIFRC® can be calculated based on the distribution of stresses caused by bending. To determine the strain distribution along the height of the section the following assumptions are made:

- Plane sections remain plane after bending. In other words, the distribution of strain through the full height of the beam is linear (Bernoulli hypothesis);
- The bond between the retrofit strips and the original beam is perfect and there is no sliding at the interface (deformation compatibility). This assumption was fully validated by tests.
- The stress distribution in concrete and CARDIFRC® strips cannot be assessed directly from the value of strain after cracking, as the constitutive relations are expressed in terms of stress-crack opening rather than stress-strain. Using the following assumptions, the evaluation of the crack opening from the strain distribution becomes possible:
- The crack opening at the tension retrofit strip (w) is the product of the strain at this level (ε_f), and an effective length of retrofit strip (L_{eff}),
- The dominant flexural crack tip is located at the level of the neutral axis. The faces of this crack open in a linear manner (Fig. 3(a)).

In fact, the strain over the effective length of retrofit strip (L_{eff}) is released in the form of a local crack. To determine L_{eff}, the length of strain-free part of the retrofit strip should be calculated. If the tensile stress carried by the cracked strips is ignored in comparison with the tensile stress transferred by the reinforcement, the shear stress at the interface is dependent on the shear stress applied by the reinforcement, as shown in Figure 3(b). Assuming the shear stress at the level of reinforcement is distributed at 45º, a length of retrofit strip (L_{eff}) is stress-free and consequently strain-free. The deformation of this length of strip is localised in the crack opening. Therefore, to

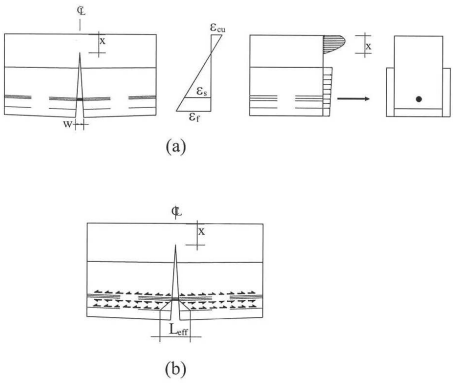

Figure. 3. (a) Modelling of the flexural crack in the middle of the beam strengthened with three strips, (b) effective length of strip for calculation of crack opening.

calculate the crack opening of the tension retrofit strip, the strain at this level (ε_f) can be multiplied by this effective length (L_{eff}) i.e. twice the distance between the reinforcement and the tension strip. It can be seen that by using this method the stress distribution in the repair material can also be worked out from the strain distribution. Due to the fact that the crack opening displacements (i.e. crack widths) of the test beams were too small for accurate measurement, the crack openings calculated from the above method could not be compared directly with measured values. However, the consequences of the above assumptions to the calculation of the moment resistance and the load deflection response of the beams will become clear when we compare the model and test results.

Figure 4 compares the maximum moment resistance of the beams predicted by the analytical model with the three- and four-point bend test results of stage I, respectively. It should be emphasised that the present model is only applicable to beams which fail in flexure.

Figure 5 compares the maximum load carrying capacity of the stage II beams (with shear reinforcement) with the model predictions. It can be seen that the model predictions are again in good agreement with the test results. Of course, the failure load of some beams retrofitted with 20mm strips is lower than that predicted by the model. This is likely to be the result of the poor quality of some 20mm strips used for retrofitting the beams.

8. SECOND ANALYTICAL MODEL

Fracture mechanics studies the response and failure of structures as a consequence of crack initiation and propagation. To model the response of a

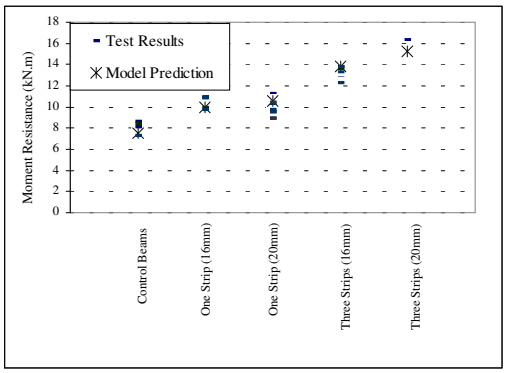

Figure. 4. Comparison of the moment resistance of the stage I beams with the predictions of the first analytical model.

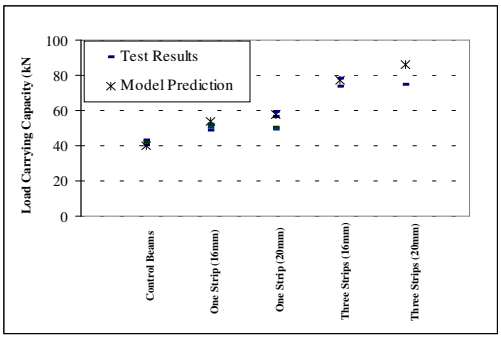

Figure. 5. Comparison of the load carrying capacity of the stage II beams with that predicted by the first analytical model.

structure based on this theory, it is therefore necessary to have a good knowledge of the details of the formation and growth of the cracks in the structure.

Let us review the sequence of the crack growth in the beams retrofitted with different configurations of retrofit strip. Of course, to model the flexural failure of the beams we will only concentrate on the behaviour of the beams, which failed in flexure and ignore those (very) few retrofitted beams that failed in shear or in a combination of shear and flexural modes.

As mentioned earlier, all the beams were pre-cracked prior to the retrofitting. During the process of pre-loading, a few flexural cracks appeared in the beams and opened up. These cracks closed (became invisible to the naked eye), when the load was removed from the beams.

After the beams were retrofitted, they were loaded again, but this time to failure. As the applied load was increased, the existing hairline cracks, induced by pre-loading, became visible again. One of these cracks in the pre-damaged beam opened and with a further increase in load this crack opened further and propagated into the tension strip. In none of the test beams was there any evidence of this crack branching into the interface. The pre-existing crack and the new crack, formed in the tension strip, continued to open until the maximum load was reached. At this stage the crack could be seen across the entire width of the tension strip. However, no attempt was made to measure the crack mouth opening displacement at the maximum load because it was too small for accurate measurement.

In the beams retrofitted with a tension strip and side strips the load increased further until the crack in the tension strip extended along the side strips. However, the crack was still within the side strips when the maximum load was reached. It extended beyond the side strips and into the concrete beam after the attainment of the maximum load.

To model the flexural failure of the retrofitted beams, let us consider the free body diagram of a part of the retrofitted beam containing the dominant flexural crack and study the effect of different loads on it (Fig. 6). It can be seen that in addition to the moment due to the applied load, there are three loads which appear in the free body diagram. The first load is due to the bridging force across the crack faces from the reinforcing steel, the second is from the post-peak tension softening response of concrete, and the third is from the bridging stresses in the retrofit strips. It is evident that only the moment tends to open the crack and the remaining loads tend to close it.

Next we relate the applied moment M to the crack depth a and crack mouth opening w.

As shown in Figure 6, closure pressures exerted by steel, concrete and retrofit strips counteract the opening action of the applied moment. As the stress at the crack tip is finite, the net stress intensity factor at the crack tip must vanish. In fact, this requires that the crack faces close smoothly near the tip. The net K_I at the crack tip is obtained by superposing the stress intensity factors produced at the crack tip by the applied moment (K_{IM}), and the closure forces exerted by steel (K_{IS}), concrete (K_{Iconc}), tension retrofit strip ($K_{I(t\text{-}strip)}$), and side retrofit strips ($K_{I(s\text{-}strip)}$) (if they are used). The condition of finite stress at crack tip, i.e. $K_I = 0$ is therefore

$$K_{IM} - K_{I\,S} - K_{I\,con\,c} - K_{I\,(t\text{-}strip)} - K_{I\,(s\text{-}strip)} = 0 \qquad (4)$$

In addition to the condition of smooth closure of crack faces at its tip, we must consider the compatibility of crack opening displacement of a retrofitted beam (Leung, 1998). The crack opening displacement can again be written as the vectorial

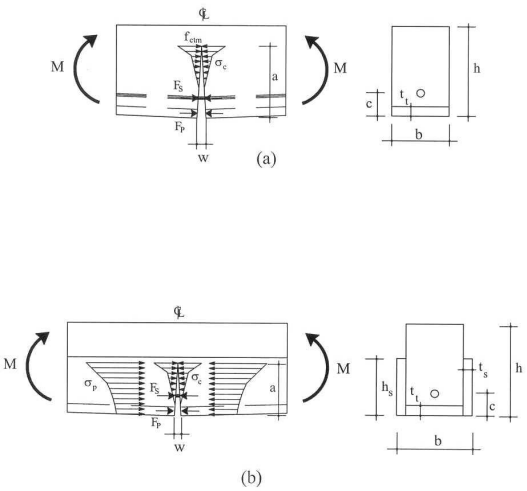

Figure 6. Free body diagram of the dominant flexural crack in retrofitted beams. Beams retrofitted with (a) one tension strip, and (b) one tension and two side strips.

sum of the contributions from the applied bending moment and the closure forces exerted by steel, concrete and retrofit strips. The compatibility condition of the crack opening need be satisfied only at the level of the steel reinforcement, because of the assumed known (i.e. linear) variation along the length of the crack:

$$(w_S)_M - (w_S)_S - (w_S)_{conc} - (w_S)_{t\text{-}strip} - (w_S)_{sstrip} = w_S \quad (5)$$

where $(w_S)_i$'s are the crack opening displacement at the level of the steel bar produced by the applied bending moment and the closure forces exerted by steel, concrete, tension strip, and side strips, respectively. Note that the crack opening w_S at the level of the reinforcement is not known, but is to be determined.

Each term in the left-hand side of (5) can be expressed in terms of the corresponding compliance coefficients. For instance, the crack opening at the level of the steel bar produced by the applied moment is

$$(w_S)_M = \bullet_{SM} M \quad (6)$$

where $\bullet_{SM}$ (the compliance coefficient) is the crack opening at the level of steel when a unit bending moment is applied to the crack. The compliance coefficients can be computed from energy principles and Clapeyron's theorem (Bosco and Carpinteri, 1992). These are listed in Alaee and Karihaloo (2002b).

As shown in the previous sections, from the fracture mechanics point of view, two equations should be simultaneously satisfied for a flexural crack; the equation of smooth closure of the crack faces (4) and the equation of the crack opening compatibility (5). The three unknown parameters in these two equations are the crack depth a, the crack mouth opening w and the applied moment M which were obtained as follows in an enumerative optimisation procedure.

- First, the equation of smooth closure of the crack faces (4) was solved for all the possible crack depths and crack mouth openings, and the corresponding moment M was calculated.
- Next, the equation of the crack opening compatibility (5) was solved for the same ranges of values of a and w.
- The results of the previous two stages were compared and the intersection of these two sets identified. This set satisfies both the smooth closure condition (4) and the crack opening compatibility equation (5).
- Among the set of values identified in the previous stage, the maximum moment was selected. In fact, this moment M_F is the moment resistance of the beam, and the corresponding crack length a and crack mouth opening w describe the condition of the dominant flexural crack at the maximum moment.

Figures 7 and 8 compare the moment resistance of the beams predicted by the model with the test results. It can be seen that the trend of the model results for both stage I and stage II beams is in agreement with the test results. It should be noted that only for the single beam retrofitted with three 20mm strips is the prediction higher than the test result. This is not surprising when one realises that this beam failed in shear. As mentioned before, the

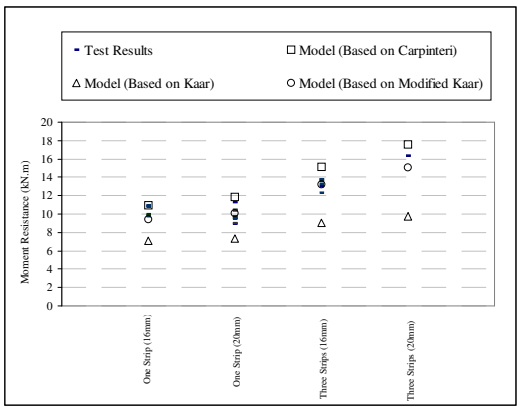

Figure 7. Comparison of the moment resistance of the stage II beams with the predictions of the second model.

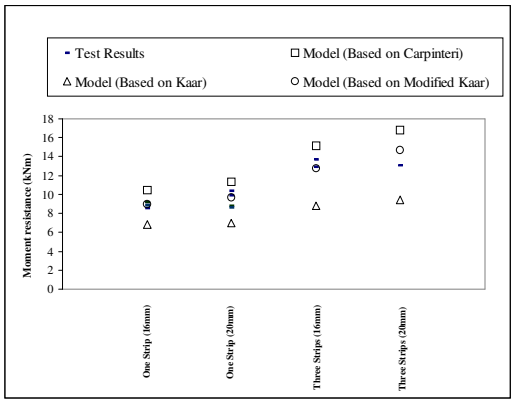

Figure 8. Comparison of the moment resistance of the stage I beams with the predictions of the second model.

model developed above is based on the behaviour of a flexural crack; it is not capable of predicting the load at which the beam fails in shear.

9. CONCLUSIONS

The new technique using the CARDIFRC® strip bonding system is a promising method for improving the flexural and shear behaviour, as well as the serviceability of damaged concrete beams. It does not suffer from the drawbacks of the existing techniques, which are primarily a result of the mis-match in the properties between the concrete and the repair material.

The mechanical properties of CARDIFRC® mixes I and II are very similar, therefore there is no real difference in the behaviour of the beams retrofitted with either of these mixes.

The moment resistance and load-deflection response of the beams retrofitted using this technique can be predicted analytically by either of the two models presented here, providing that the strain hardening and tension softening response of concrete and CARDIFRC® are properly taken into account.

The technique described in this paper may be used when there is a need to improve the durability of existing concrete structures, as CARDIFRC® mixes are very durable because of their highly dense microstructure. Research is currently being undertaken to study the fatigue, shrinkage and creep properties of CARDIFRC® and the performance of concrete structures retrofitted with CARDIFRC® under dynamic, thermal and hygral loads.

10. ACKNOWLEDGEMENT

This work is supported by the UK EPSRC grant GR/R11339.

11. REFERENCES

Ahmed O. & Gemert D. V. 1999. Behaviour of R.C. beams strengthened in bending by CFRP laminates. *Proceedings of Structural faults & repair – 99:8th International Conference*, London, CD-Rom.

Alaee, F. J., Benson, S. D. P. & Karihaloo B. L. 2002. High-Performance Cementitious Composites for Retrofitting, *International Journal of Materials and Product Technology*, 17(1/2): 17-31.

Alaee, F. J. & Karihaloo B. L. 2003a. Retrofitting of RC beams with CARDIFRC®. *ASCE Journal of Composites for Construction,* 7:174-186.

Alaee, F. J. & Karihaloo B. L. 2003b. Fracture model for flexural failue of beams retrofitted with CARDIFRC®. *ASCE Journal of Engineering mechanics*, 129:1028-1038.

Büyüköztürk O. & Hearing B. 1998. Failure behaviour of precracked concrete beams with FRP. *Journal of Composites for Construction*, ASCE, 2(3): 138-144.

CEB-FIP Model Code. 1993. Lausanne, Switzerland.

El-Refaie S. A., Ashour A. F. & Garrity S. W. 1999. Flexural capacity of R.C. beams strengthened with external plates. *Proceedings of Structural faults & repair – 99:8th International Conference*, London, CD-Rom.

Karihaloo B. L., Alaee, F. J. & Benson, S. D. P. 2002. A New Technique for Retrofitting Damaged Concrete Structures, *Proceedings of the Institution of Civil Engineers, Buildings & Structures,* 152(4): 309-318.

Karihaloo B. L., Benson S. D. P., Didiuk P. M., Fraser S. A., Hamill N. & Jenkins T. A. 2000. Retrofitting damaged RC beams with high-performance fibre-reinforced concrete. *Proceedings of Concrete Communication Conference*, British Cement Association, Birmingham, 153-164.

Karihaloo, B.L. & Jefferson, A.D. 2001. Looking into concrete, *Magazine of Concrete Research*, 53: 135-147.

Karihaloo, B.L. & Wang, J. 2000. Constitutive modelling of high performance fibre-reinforced cementitious composites, *Journal of Advanced Engineering Materials*, 2: 726-732.

Karihaloo, B.L., Wang, J. & Grzybowski, M.. 1996. Doubly periodic arrays of bridged cracks and short-fibre-reinforced cementitious composites, *Journal of the Mechanics and Physics of Solids,* 44: 1656-1586.

Leung, C. K. Y. 1998. Delamination Failure in Concrete Beams Retrofitted with a Bonded Plate. In *Fracture Mechanics of Concrete Structures,* Mihashi, H., Rokugo, K. (eds), AEDIFICATIO Publishers, Freiburg, Germany, 3:1783-1792.

Nanni A. 1995. Concrete repair with externally bonded FRP reinforcement: examples from Japan. *Concrete International*, 97: 22-26.

Neuber, H. 1969. Der Zugbeanspruchte Flachstab mit optimalem Querschnittsübergang, *Forschung im Ingenieurwesen*, 35: 29-30.

Wang, J. Fang, J. & Karihaloo, B.L. 2000. Asymptotics of multiple crack interactions and prediction of effective modulus, *International Journal of Solids and Structures*, 37: 4261-4273.